Available online at www.sciencedirect.com
ScienceDirect
Acta Materialia 57 (2009) 1–7
Acta MATERIALIA
www.elsevier.com/locate/actamat

Mechanism for the development of anisotropic grain boundary character distributions during normal grain growth

Shen J. Dillon *, Gregory S. Rohrer

Department of Materials Science and Engineering, Carnegie Mellon University, 5000 Forbes Avenue, Pittsburgh, PA 15213-3890, USA

Received 11 June 2008; received in revised form 22 August 2008; accepted 22 August 2008
Available online 6 October 2008

Abstract

Grain boundaries in polycrystalline magnesia-doped alumina and yttrium aluminum garnet were classified as growing in area or shrinking in area on the basis of topology and curvature considerations. Measurements of dihedral angles at grain boundary thermal grooves were used to determine that the energies of the growing boundaries are, on average, lower than the energies of the shrinking boundaries. The observations also show that the length of a boundary is inversely correlated to its energy. The findings suggest that anisotropic grain boundary character distributions, which influence the properties of polycrystals, develop because higher-energy grain boundaries are preferentially eliminated from the network during grain growth.

Keywords: Grain boundaries; Grain boundary energy; Grain boundary migration; Misorientation

1. Introduction

A number of experimental and theoretical studies in the past decade have shown that polycrystalline materials develop an anisotropic grain boundary character distribution (GBCD) during grain growth [1–21]. The GBCD is the relative areas of grain boundaries distinguished by their lattice misorientations and grain boundary plane orientations. Results from experiment and simulation suggest that there is an inverse relationship between the relative energy of a grain boundary and its total area in the polycrystal [8,10,22–24]. Measurements have shown that in $SrTiO_3$ the most common grain boundaries in the distribution are both more numerous and have larger average areas than others [25]. The GBCD and its mechanistic origin are of interest because the grain boundary network can affect bulk properties such as the mechanical response, transport kinetics or corrosion resistance [21,26–37]. This point is exemplified by the widespread interest in grain boundary engineering [26–29,31,34–43]. Although the GBCD is thought to be a sensitive indicator of materials properties and that it is possible to engineer a polycrystal by controlling the GBCD, little is known about the mechanism of how anisotropic distributions develop.

Simulations of grain growth have shown that the anisotropic GBCD results from anisotropy in the grain boundary energy rather than from anisotropic grain boundary mobilities [22–24]. Holm et al. [23] simulated anisotropic grain growth and found that, in untextured microstructures, the mean area of low-energy grain boundaries was larger than high-energy boundaries. They also found that the relative numbers of different boundary types did not vary significantly with energy, and suggested that the observed behavior was due to the preferential lengthening of low-energy grain boundaries. A geometric mechanism was proposed based on the force balance at triple junctions, where low-energy boundaries (relative to their neighbors) have a larger dihedral angle and preferentially lengthen at the expense of higher-energy boundaries, which preferentially shrink [23]. While this grain boundary-lengthening model accounts for anisotropy in the average areas of different grain boundary types, it does not explain

* Corresponding author.
E-mail address: sjd6@lehigh.edu (S.J. Dillon).

1359-6454/$34.00 © 2008 Acta Materialia Inc. Published by Elsevier Ltd. All rights reserved.
doi:10.1016/j.actamat.2008.08.062

the observed anisotropy in the numbers of different grain boundary types. More recently, the anisotropy in the numbers and average areas of different grain boundary types was observed in a three-dimensional Monte Carlo simulation [22].

Based on these observations, a model was recently proposed to explain the evolution of the anisotropic GBCD to a steady state during normal grain growth [44]. The model adopts the proposal made by Holm et al. [23], that energies influence the relative areas of grain boundaries by changing the geometries of triple junctions. The relative numbers of different grain boundary types must be changed through critical topological events, such as the elimination of a grain boundary face. Therefore, it was assumed that the probability that a critical event annihilates a particular type of grain boundary is directly proportional to the relative number of these boundaries and inversely proportional to the average area of such boundaries. The probability that a particular type of grain boundary is created by a grain impingement event is taken to be a random combination of the available orientations. Using these assumptions about the creation and annihilation probabilities for grain boundaries with anisotropic energies, it was shown that random GBCDs evolve to steady state distributions that are inversely related to the grain boundary energy anisotropy. We refer to this as the critical event (CE) model [44].

While the CE model produces results that are in good agreement with experiment, it is based on two assumptions that have not been experimentally demonstrated: that higher-energy grain boundaries have, on average, smaller areas than lower-energy grain boundaries and that the probability of a higher-energy grain boundary being eliminated in a critical event is greater than that of a lower-energy grain boundary. The purpose of this paper is to test these assumptions. Relative grain boundary energies are evaluated using thermal groove measurements. While we cannot directly measure the probability of elimination of a boundary, we can determine whether the area of a grain boundary is shrinking or growing and, therefore, the distributions of the energies and lengths of shrinking grain boundaries can be compared to those of growing grain boundaries. The observations reported here are consistent with the assumptions of the CE model and suggest that the energy biased elimination of grain boundaries during normal grain growth is a plausible mechanism for the development of anisotropic GBCDs.

2. Methods

Assuming the mean curvature of the interface is in the same direction as the principal curvature of the trace observed in the planar section, the sign of the curvature identifies the direction of motion. Each boundary in a plane section is connected to four other boundaries and there are seven different possible curvature configurations for the four connecting boundaries (see Fig. 1). When all four boundaries are concave (Type A), we can be certain

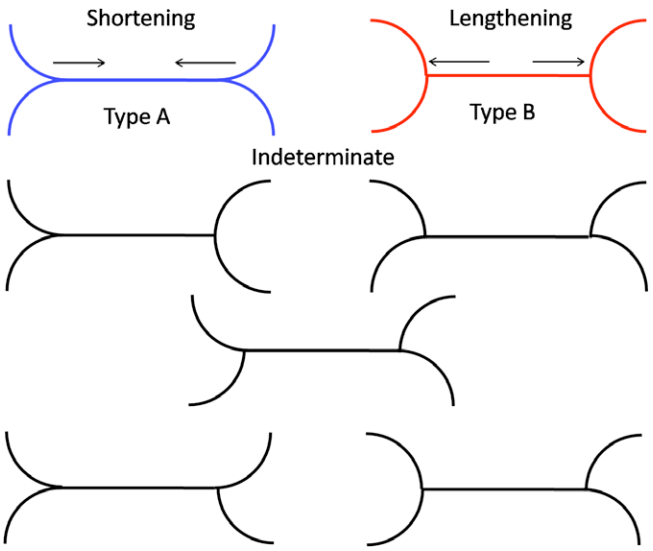

Fig. 1. Schematic of seven different grain boundary topologies based on the curvature of the adjacent grain boundaries.

that both triple junctions were moving toward one another and that the central boundary was decreasing in area before annealing was interrupted. This will be referred to as a shrinking grain boundary. When all four boundaries are convex (Type B), we can be certain both triple junctions are moving away from one another and that central boundary was increasing in area. This will be referred to as a growing boundary. The situation for the remaining five cases is uncertain. Therefore, based on the curvatures of its four connecting grain boundaries, any boundary can be classified as shrinking, growing or uncertain. It is then possible to measure the relative grain boundary to surface energy distributions of each of these three classes by measuring the dihedral angles from thermal grooves. Some grain boundaries appear to be relatively straight and the curvature of these boundaries must be approximated to the best of the observer's ability. However, if three of the adjacent boundaries show consistent curvature and the fourth is approximately straight, the direction of motion is still predictable.

Magnesia-doped alumina was prepared with the nominal composition of 500 ppm MgO, as described in detail elsewhere [45]. The sample was polished to a 1 μm diamond finish and subsequently thermally etched at 1400 °C for 2 h to produce thermal grooves at the grain boundaries. Commercially available transparent yttrium aluminum garnet (YAG) (Baikowski International Corp., NC) was polished and thermally etched at 1300 °C for 2 h to produce thermal grooves. Both samples had equiaxed grains.

Electron backscatter diffraction (EBSD) in the scanning electron microscope (XL 40, FEI Company) was used to characterize the orientations of more than 20,000 grains in each sample. The area weighted average grain size of the alumina was 2.5 μm, and the EBSD data was collected at a step size of 0.15 μm. The area weighted average grain size of the YAG was 2.8 μm, and the EBSD data was col-

lected at a step size of 0.25 μm. Both data sets were cleaned using three iterations of grain dilation with a minimum grain size of 10 pixels. The traces of the grain boundaries were determined using OIM software (TexSEM Laboratories Inc.) using a maximum deviation of 2 pixels between the trace and the true boundary position. The distributions of grain boundary plane orientations, independent of misorientation, were calculated using a stereological technique that has been described in detail elsewhere [9].

An atomic force microscope (AFM) (CP-II, Veeco) was used in contact mode to measure the topographies of grain boundary thermal grooves. The geometry of the thermal groove can be used to extract the surface dihedral angle (Ψ_S) from the height (d) and width (W) of the grain boundary, using Mullins's analysis [46]. A schematic of a thermal groove is shown in Fig. 2. The dihedral angle is related to the ratio of the grain boundary energy (γ_{GB}) to surface energy (γ_S) through the following equation:

$$\frac{\gamma_{GB}}{\gamma_S} = 2\cos\left(\frac{\Psi_S}{2}\right) \quad (1)$$

The groove measurements were made using previously described procedures [47]. Briefly, three measurements of each groove were used to calculate an average dihedral angle and standard deviation. A scan resolution between 2 and 10 nm per pixel was used.

The radius of curvature of the AFM tip can introduce artifacts into the thermal groove profiles. Saylor et al. [47] considered this effect and calculated the error as a function of the groove width and dihedral angle. Using the results in Ref. [47] as a guide, the average dihedral angles of the alumina and YAG studied here are at most overestimated by up to 7° and 2°, respectively. Note that this error is systematic and does not introduce trends into the data, but may instead slightly offset the mean of each population in the same direction.

The analysis of individual grooves is also complicated by the fact that the inclination of the grain boundary is not known, and that the surface energy anisotropy is not known. However, when a large population of grain boundaries is measured, it is possible to average over these effects because the grain boundary inclination angles and surface orientations are randomly distributed. When measuring two distinct populations of grain boundaries, the surface effect and grain boundary inclination effect should, on average, be equivalent within a given sample. It is then possible to isolate the average effect of the grain boundary energy on the dihedral angles of the growing and shrinking boundaries.

A representative AFM image highlighting examples of a growing and shrinking grain boundary is shown in Fig. 3a. Corresponding line profiles across these two boundaries are shown in Fig. 3b. The dihedral angles of more than 500 thermal grooves in magnesia-doped alumina were measured so that there were at least 100 boundaries representing each of the three grain boundary types. The grain boundary length was also measured, where length is taken as the distance between triple junctions. Because some

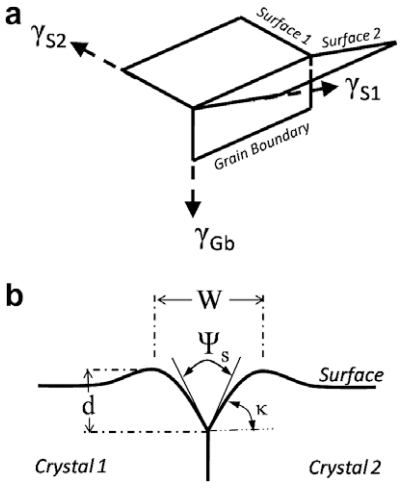

Fig. 2. Schematic of thermal groove geometry. (a) An oblique projection of the junction. (b) A two-dimensional section perpendicular to the triple line.

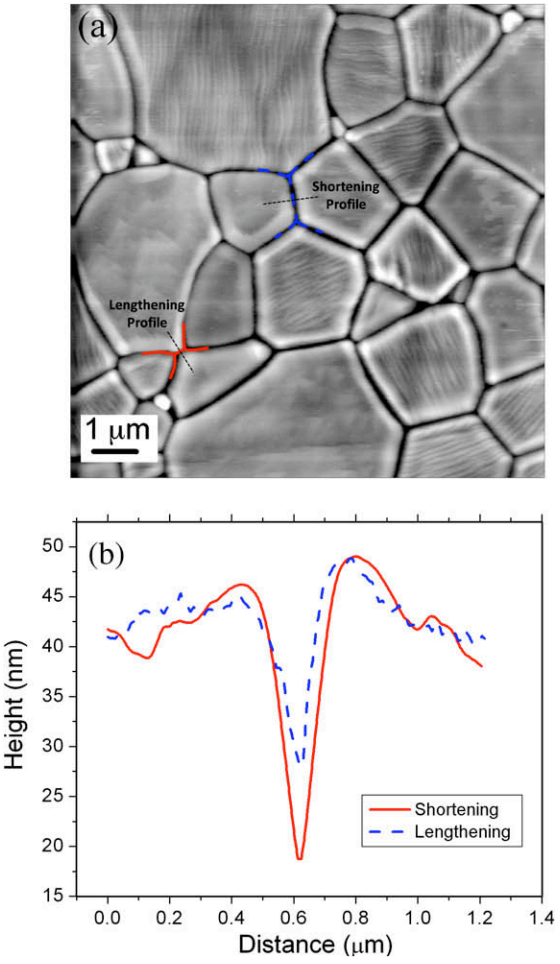

Fig. 3. (a) AFM image of a YAG sample showing a lengthening (dotted) and shortening (solid) grain boundary outlined. (b) The corresponding thermal groove profiles.

grain boundaries are curved, this slightly underestimates the true length of those boundaries.

3. Results

The distributions of grain boundary plane normals in the crystal reference frame, in units of multiples of a random distribution (MRD), are shown in Fig. 4. The magnesia-doped alumina is anisotropic and shows a preference for (0 0 0 1) basal planes. This is known to be a low-energy plane in alumina [48]. The YAG is more isotropic with preference for (1 1 0) planes and (1 1 1) planes. The difference between the maximum and minimum of the alumina distribution (0.31 MRD) is approximately twice that of the YAG distribution (0.14 MRD).

Fig. 5 shows the average dihedral angle plotted against the average grain boundary length for grain boundaries whose lengths have been classified into 200 nm wide bins. This plot shows a direct correlation between grain boundary length and grain boundary energy. The longest grain boundaries have, on average, lower relative energies. It should be noted that these data are subject to stereological affects associated with observing a two-dimensional section of a three-dimensional microstructure. It is well known

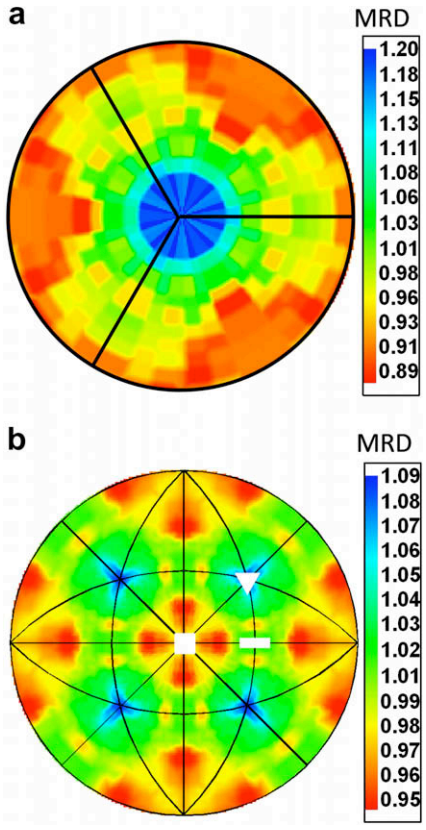

Fig. 4. The distribution of grain boundary plane orientations, in the crystal reference frame, expressed in multiples of random, for (a) magnesia-doped alumina annealed for 2 h at 1400 °C and (b) YAG annealed for 2 h at 1300 °C. The square, rectangle and triangle indicate the (1 0 0), (1 1 0) and (1 1 1) planes, respectively.

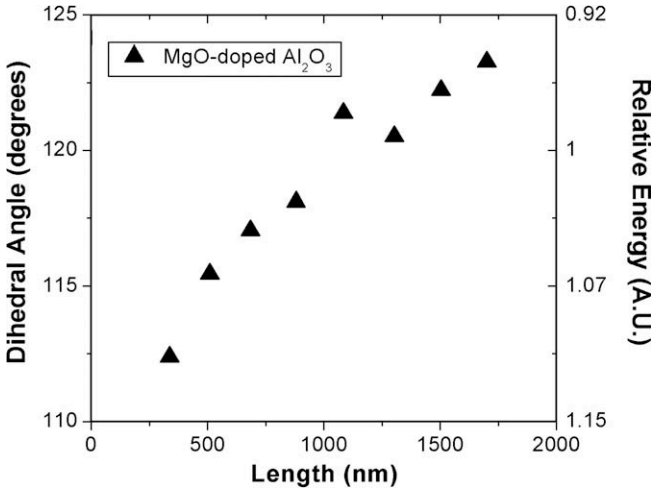

Fig. 5. The relationship between average distance between adjacent triple junctions (grain boundary length) and the relative grain boundary energy.

that on average the grain boundary length observed in plane section scales with the true grain boundary area [49]. However, classifying the data in discrete bins distorts this relationship. For example, sections of some large area grain boundaries will be sorted into bins with short-grain boundaries. This should cause the short-grain boundary end of the distribution to be slightly skewed towards lower energies than the real population. This tends to suppress the trend in the relationship between grain boundary area and grain boundary energy and, therefore, does not alter the conclusion that a clear trend exists.

The distributions of thermal grooves for growing and shrinking grain boundaries are shown in Fig. 6, along with data for a randomly selected population. The median dihedral angle of the shrinking, random, and growing grain boundary distributions in the magnesia-doped alumina are 102°, 116° and 128°, respectively. Handwerker et al. [50] reported a median dihedral angle of 117° and this is consistent with the value observed here for the random population (116°). The median dihedral angles for the shrinking, random, and growing grain boundaries in YAG are 155°, 158° and 160°, respectively. Based on a previously reported image of a thermal groove at the Σ5 twist grain boundary in YAG, we conclude that the dihedral angle of this boundary is approximately 145° [51]. This is consistent with, but in the higher-energy range of, the distribution observed here. The population of this boundary in the GBCD is less than 1 MRD, which is consistent with a higher-energy grain boundary.

The differences in the median relative grain boundary to surface energy ratios between the growing and shrinking boundaries is 44% and 25% for the magnesia-doped alumina and YAG, respectively. The widths of these distributions correlate with the measured anisotropy in the grain boundary plane distributions (see Fig. 4). In other words, the sample with the widest distribution of energies has the more pronounced grain boundary plane texture.

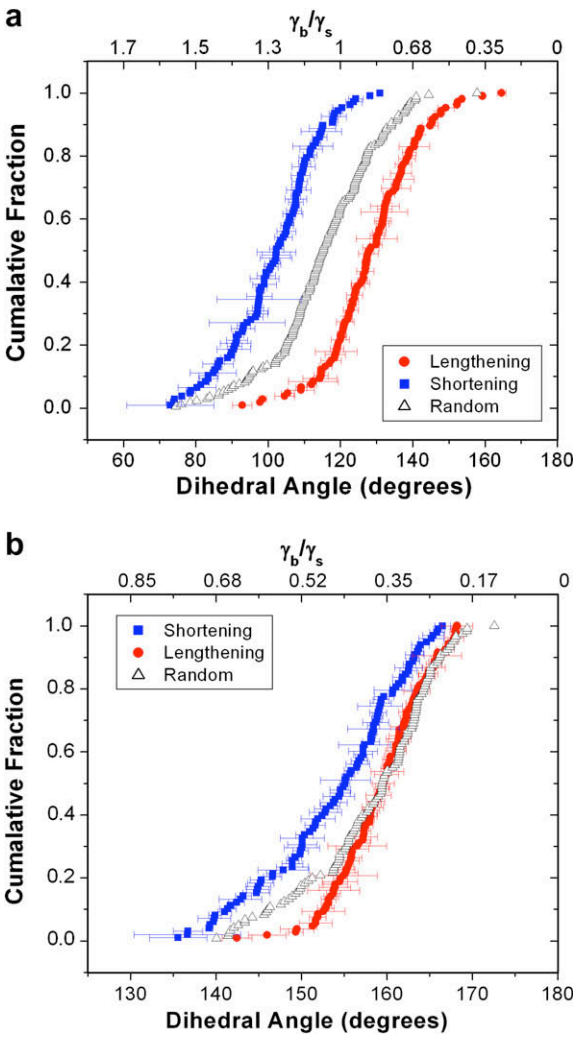

Fig. 6. Distribution of dihedral angles for lengthening, shortening, and random grain boundaries in (a) magnesia-doped alumina and (b) YAG. The error bars represent the standard deviation from three measurements on each boundary.

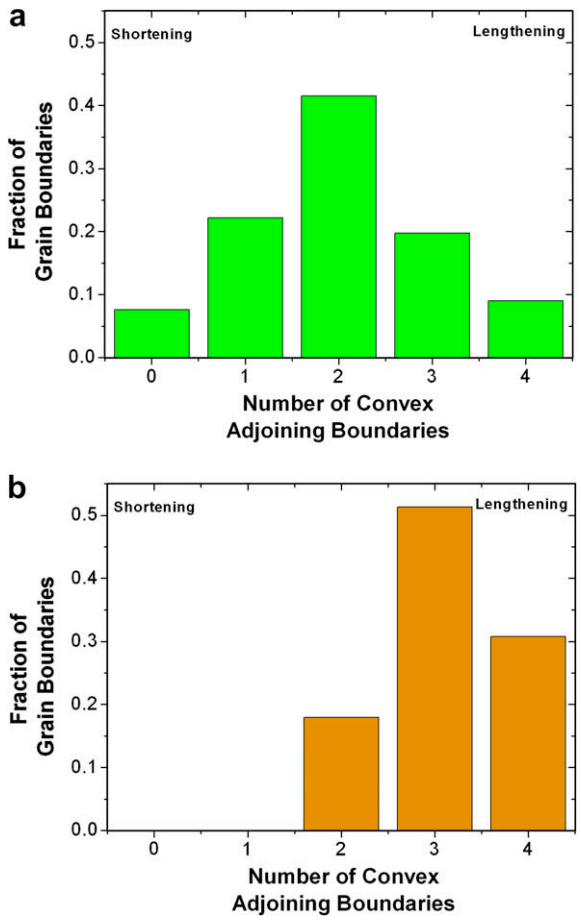

Fig. 7. The fraction of grain boundaries with convex adjoining grain boundaries for (a) ~300 random grain boundaries and (b) 36 "low-energy" grain boundaries.

The data in Fig. 7a shows the distribution of boundary types, where the type is defined as the number of attached convex boundaries. The distribution is based on the observation of 300 random YAG grain boundaries, observed with no prior knowledge of their orientations. In this distribution, boundaries with four adjacent, convex neighbors are growing. The distribution appears to be symmetric with approximately the same number of boundaries growing and shrinking in area. We can compare the distribution of random GB types in Fig. 7a to the distribution of boundaries assumed to have relatively low-energy (Fig. 7b). EBSD data was used to identify 36 boundaries that were Σ1, Σ3 or Σ9 (classified using the conventional coincident site classification). These boundaries have two, three, or four attached grain boundaries that are convex. A comparison of the distributions in Fig. 7a and b suggests that low-Σ CSL boundaries, which are often assumed to have relatively low-energies, are more likely to be growing in area rather than shrinking. It should be noted that while we cannot be certain that all of the low-Σ CSL boundaries have relatively low-energies, we are confident that the Σ1 grain boundaries have relatively low-energies and these comprise 56% of the data set.

4. Discussion

The objective of this work was to experimentally support the hypothesis that anisotropic grain boundary character distributions, in which high-energy grain boundaries are found less frequently than low-energy grain boundaries, develop from random distributions during normal grain growth by the preferential elimination of the high-energy grain boundaries. The rationale for this is that during grain growth, some grain boundaries are eliminated when two grains separate or a tetrahedral grain disappears, while others are created when two grains impinge. Because grain growth leads to a reduction in the total interfacial area, more grain boundaries must be eliminated than created. If the polycrystal is composed of randomly oriented grains, then the distribution of grain boundaries created by impingement should be random. It must therefore be the preferential elimination of high-energy boundaries

that leads to a higher relative population of low-energy grain boundaries.

While it is not possible to measure the frequency with which different boundaries are eliminated, it is possible to determine which grain boundaries are shrinking and which are growing. Based on their thermal grooves, growing boundaries have relatively lower energies. Also, boundaries thought to be low-energy (low Σ CSL boundaries) are more likely to be growing. Therefore, assuming that shrinking boundaries are more likely to be eliminated than growing boundaries, the results are consistent with the idea that higher-energy grain boundaries are eliminated with a probability that is greater than lower-energy grain boundaries. This is also reflected in the areas of the boundaries. The lower-energy boundaries, that are growing, have larger average areas than the higher-energy boundaries. Therefore, the principal assumptions of the CE model are justified by observation.

The current results show that there is a preference for the direction of triple junction motion based on the relative energy of the intersecting grain boundaries and this complements the grain boundary-lengthening mechanism advocated in the CE model [44]. The direction of triple junction motion is inherently linked to the dihedral angle (Ψ_b) of those grain boundaries. This point is illustrated in Fig. 8, which shows an idealized pair of triple junctions separated by the angle β, measured relative to the center of the grain. This angle is related to the dihedral angles of the pair of triple junctions by the following simple geometric relationship:

$$\beta - \frac{\Psi_{b1} - \Psi_{b2}}{2} = \pi \tag{2}$$

When this equation is satisfied in two dimensions, the grain boundaries will be stable and the triple junctions will not move. If the left-hand side of the equation is larger than π, then grain boundaries 1 and 2 will tend to lengthen or grow. Note that large dihedral angles are expected for relatively low-energy boundaries. Alternatively, when the dihedral angles or β are small, these grain boundaries tend to shrink or shorten. Small dihedral angles are expected when grain boundaries 1 and 2 have relatively high energies. Therefore, the trend in the grain boundary-lengthening model matches our experimental results and the mechanism for both effects relate directly to the grain boundary dihedral angle.

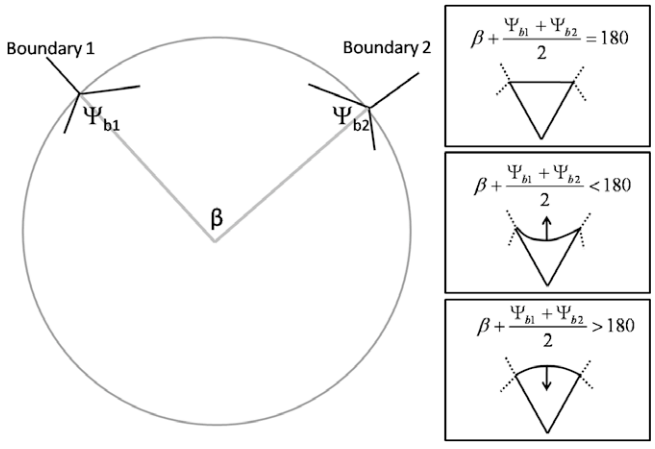

Fig. 8. Schematic of a set of idealized triple junctions showing the effect of their geometry on the direction of curvature of the grain boundary linking them.

It is worth emphasizing that the trends discussed here occur on average, but not in every case. For example, as a polycrystal evolves to a single crystal, every boundary is at some point decreasing in area, regardless of its energy. Furthermore, as grain growth is active, new high-energy grain boundaries are continually injected into the system by grain impingement events. The importance of local phenomena in determining the behaviors of individual boundaries is illustrated by Eq. (2), which depends on the energies of the adjoining boundaries (which influence Ψ_b) and the local grain coordination (which influences β). The direction of triple junction motion will also be influenced by critical topological events occurring at the neighboring junctions by changing the energies of the adjoining grain boundaries and the coordination of the surrounding grains.

The proposed mechanism for the development of anisotropic GBCDs is envisioned to apply to polycrystals evolving by normal grain growth. When microstructures evolve by abnormal grain growth, certain boundaries move and grow at rates many times faster than their neighbors. The selection of such boundaries may not be related to energy, at least in the same manner. Similarly, when microstructures are evolving under the influence of stored plastic energy (for example, during recrystallization or grain boundary engineering processes) it is not obvious that grain boundary energy would be the deciding factor in determining which boundaries are shrinking or growing. However, microstructures that evolve in this way do lead to anisotropic GBCDs that appear to emphasize low-energy grain boundaries [1,2,52,53]. Developing a complete understanding of how the grain boundary character evolves will enable new strategies for tailoring materials properties.

5. Conclusion

Lower-energy boundaries have, on average, larger areas than higher-energy boundaries. Low-energy boundaries also tend to increase in area, while high-energy boundaries tend to decrease in area. These two phenomena lead to the development of an anisotropic GBCD. The difference between the average grain boundary energy of the population whose grain boundary area is increasing and the average energy of the population whose grain boundary area is decreasing correlates with the amount of anisotropy observed in the GBCD. The link between a grain boundary's energy and its tendency to be eliminated from the distribution provides a fundamental new mechanism for the development of interfacial anisotropy during grain growth.

Acknowledgements

This work was supported the Pennsylvania DCED and by the MRSEC program of the National Science Foundation under Award Number DMR-0520425.

References

[1] Bennett TA, Kim C-S, Rohrer GS, Rollett AD. Mater Sci Forum 2004;467–470:727.
[2] Gorzkowski EP, Sano T, Kim C-S, Rohrer GS, Chan HM, Harmer MP. Z Metall 2005;96:207.
[3] Kim C-S, Rohrer GS. Interface Sci 2004;12:19.
[4] Kim C-S, Rollett AD, Rohrer GS. Scripta Mater 2006;54:1005.
[5] Miller HM, Saylor DM, El Dasher BS, Rollett AD, Rohrer GS. Mater Sci Forum 2004;467–470:783.
[6] Randle V, Rohrer GS, Hu Y. Scripta Mater 2008;58:183.
[7] Rohrer GS, Randle V, Kim C-S, Hu Y. Acta Mater 2006;54:4489.
[8] Saylor DM, El Dasher B, Pang Y, Miller HM, Wynblatt P, Rollett AD, et al. J Am Ceram Soc 2004;87:724.
[9] Saylor DM, El-Dasher BS, Adams BL, Rohrer GS. Metall Mater Trans A 2004;35A:1981.
[10] Saylor DM, Morawiec A, Rohrer GS. Acta Mater 2003;51:3675.
[11] Pang Y, Wynblatt P. J Am Ceram Soc 2006;89:666.
[12] Bozzolo N, Sawina G, Gerspach F, Sztwiertnia K, Rollett AD, Wagner F. Mater Sci Forum 2007;558–559:863.
[13] Garcia RE, Vaudin MD. Acta Mater 2007;55:5728.
[14] Homer ER, Adams BL, Wagoner RH. Metall Mater Trans A 2007;38A:1575.
[15] Bhattacharjee PP, Sinha SK, Upadhyaya A. Scripta Mater 2006;56:13.
[16] Tsurekawa S, Nakamichi S, Watanabe T. Acta Mater 2006;54:3617.
[17] Homer ER, Adams BL, Fullwood DT. Scripta Mater 2006;54:1017.
[18] Lee S-L, Richards NL. Mater Sci Eng A 2005;A405:74.
[19] Schuh CA, Kumar M, King WE. J Mater Sci 2005;40:847.
[20] Li D, Wright SI, Boehlert CJ. Scripta Mater 2004;51:545.
[21] Farooq MU, Klement U. J Microsc 2004;213:306.
[22] Gruber J, Ph.D. Thesis. Carnegie Mellon University, 2007.
[23] Holm EA, Hassold GN, Miodownik MA. Acta Mater 2001;49:2981.
[24] Kinderlehrer D, Livshits I, Rohrer GS, Ta'asan S, Yu P. Mater Sci Forum 2004;467–470:1063.
[25] Saylor DM, El Dasher B, Sano T, Rohrer GS. J Am Ceram Soc 2004;87:670.
[26] Kobayashi S, Inomata T, Kobayashi H, Tsurekawa S, Watanabe T. J Mater Sci 2008;43:3792.
[27] Tan L, Sridharan K, Allen TR, Nanstad RK, McClintock DA. J Nucl Mater 2008;374:270.
[28] Chen Y, Schuh CA. Phys Rev B 2007;76:064111/1.
[29] Kokawa H, Shimada M, Michiuchi M, Wang ZJ, Sato YS. Acta Mater 2007;55:5401.
[30] Wynblatt P, Shi Z. J Mater Sci 2005;40:2765.
[31] Watanabe T, Tsurekawa S. Mater Sci Eng A 2004;A387–A389:447.
[32] Molodov DA, Shvindlerman LS, Gottstein G. Z Metall 2003;94:1117.
[33] Tsurekawa S, Watanabe T. Diffusion Defect Data Solid State Data B Solid State Phenom 2003;93:333.
[34] Tsurekawa S, Watanabe T, Watanabe H, Tamari N. Key Eng Mater 2003;247:327.
[35] Hirata T, Tanabe S, Kohzu M, Higashi K. Scripta Mater 2003;49:891.
[36] Shimada M, Kokawa H, Wang ZJ, Sato YS, Karibe I. Acta Mater 2002;50:2331.
[37] Kim SH, Erb U, Aust KT, Palumbo G. Scripta Mater 2001;44:835.
[38] Randle V. Acta Mater 2004;52:4067.
[39] Tan L, Sridharan K, Allen TR. J Nucl Mater 2007;371:171.
[40] Lewis AC, Bingert JF, Rowenhorst DJ, Gupta A, Geltmacher AB, Spanos G. Mater Sci Eng A 2006;A418:11.
[41] Molodov DA, Konijnenberg PJ. Scripta Mater 2006;54:977.
[42] Lee SL, Richards NL. Mater Sci Eng A 2005;A390:81.
[43] Davies H, Randle V. Mater Sci Technol 2000;16:1399.
[44] Rohrer GS, Gruber J, Rollett AD. Ceram Trans 2008;201:343.
[45] Dillon SJ, Tang M, Carter WC, Harmer MP. Acta Mater 2007;55:6208.
[46] Mullins WW. J Appl Phys 1957;28:333.
[47] Saylor DM, Rohrer GS. J Am Ceram Soc 1999;82:1529.
[48] Kitayama M, Glaeser AM. J Am Ceram Soc 2002;85:611.
[49] Underwood EE. Quantitative stereology. Reading, MA: Addison-Wesley; 1981.
[50] Handwerker CA, Dynys JM, Cannon RM, Coble RL. J Am Ceram Soc 1990;73:1371.
[51] Peters MI, Reimanis IE. J Am Ceram Soc 2003;86:870.
[52] Miller HM, Kim CS, Gruber J, Randle V, Rohrer GS. Mater Sci Forum 2007;558–559:641.
[53] Sano T, Kim C-S, Rohrer GS. J Am Ceram Soc 2005;88:993.